AD-A181 289 TOMOGRAPHIC INVESTIGATIONS AT LANDFILL 4 HILL AIR FORCE 1/1
BASE LAYTON UTAH..(U) WESTON GEOPHYSICAL CORP
WESTBOROUGH MA G M JONES ET AL. 23 APR 87 SCIENTIFIC-1
UNCLASSIFIED AFGL-TR-87-0055 F19628-84-C-0130 F/G 8/10 NL

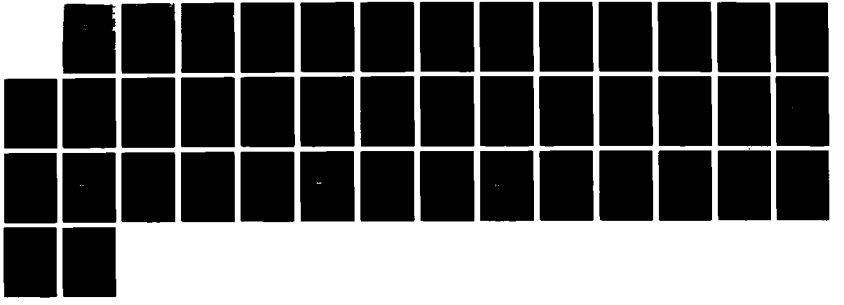

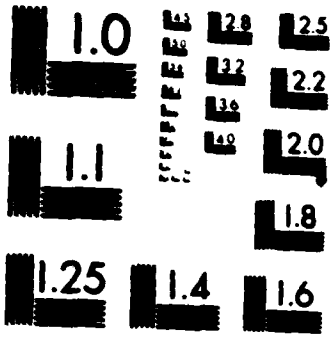

MICROCOPY RESOLUTION TEST CHART
NATIONAL BUREAU OF STANDARDS 1963 A

AFGL-TR-87-0055

TOMOGRAPHIC INVESTIGATIONS AT LANDFILL 4, HILL AIR FORCE BASE, LAYTON, UTAH

Glyn M. Jones
Vincent J. Murphy

Weston Geophysical Corporation
Post Office Box 550
Lyons Street
Westboro, Massachusetts 01581

23 April 1987

Scientific Report No. 1

AIR FORCE GEOPHYSICS LABORATORY
AIR FORCE SYSTEMS COMMAND
UNITED STATES AIR FORCE
HANSCOM AIR FORCE BASE, MASSACHUSETTS 01731

REPORT DOCUMENTATION PAGE

1a. REPORT SECURITY CLASSIFICATION Unclassified	1b. RESTRICTIVE MARKINGS
2a. SECURITY CLASSIFICATION AUTHORITY	3. DISTRIBUTION/AVAILABILITY OF REPORT Approved for public release; distribution unlimited.
2b. DECLASSIFICATION/DOWNGRADING SCHEDULE	
4. PERFORMING ORGANIZATION REPORT NUMBER(S)	5. MONITORING ORGANIZATION REPORT NUMBER(S) AFGL-TR-87-0055
6a. NAME OF PERFORMING ORGANIZATION Weston Geophysical Corporation 6b. OFFICE SYMBOL (If applicable)	7a. NAME OF MONITORING ORGANIZATION Air Force Geophysics Laboratory
6c. ADDRESS (City, State and ZIP Code) Post Office Box 550, Lyons Street Westboro, Massachusetts 01581	7b. ADDRESS (City, State and ZIP Code) Hanscom AFB Massachusetts 01731
8a. NAME OF FUNDING/SPONSORING ORGANIZATION Air Force Geophysics Laboratory 8b. OFFICE SYMBOL (If applicable)	9. PROCUREMENT INSTRUMENT IDENTIFICATION NUMBER F19628-84-C-0130
8c. ADDRESS (City, State and ZIP Code) Hanscom AFB, Massachusetts 01731	10. SOURCE OF FUNDING NOS. PROGRAM ELEMENT NO. 65502F; PROJECT NO. 5502; TASK NO. 01; WORK UNIT NO. AB
11. TITLE (Include Security Classification) Tomographic Investigations at Landfill 4, Hill AFB, Layton, Utah	
12. PERSONAL AUTHOR(S) Glyn M. Jones and Vincent J. Murphy	
13a. TYPE OF REPORT Scientific Report #1 13b. TIME COVERED FROM 11/03/86 TO 11/07/86	14. DATE OF REPORT (Yr., Mo., Day) 87-04-23 15. PAGE COUNT 42
16. SUPPLEMENTARY NOTATION	
17. COSATI CODES FIELD / GROUP / SUB. GR.	18. SUBJECT TERMS (Continue on reverse if necessary and identify by block number) Tomography, soil velocities, waste isolation, ground-water.

19. ABSTRACT (Continue on reverse if necessary and identify by block number)

In support of soil classification objectives related to an ongoing study of non-linear soil response, tomographic techniques were developed and tested using seismic data. The data were collected at three locations at Landfill 4, Hill AFB, Utah. The site is a land-fill waste site which had been isolated from the prevailing ground-water flow by a slurry trench. The objective of this study was to identify the effectiveness of geophysical techniques for seismic velocity measurements and tomographic/imaging analyses.

Seismic data were collected between pairs of 50 ft. deep boreholes on either side of the slurry trench. First break picks were analyzed using an iterative back-projection tomographic technique utilizing curved rays. Initial processing revealed that smearing of velocity anomalies between the boreholes occurred because of non-optimum placement of shots and receivers. Adding reasonable constraints to the inversion, however, showed a low-velocity region, terminating between 35 and 40 ft., at the trench location.

CONTINUED OVER

20. DISTRIBUTION/AVAILABILITY OF ABSTRACT UNCLASSIFIED/UNLIMITED ☒ SAME AS RPT. ☐ DTIC USERS ☐	21. ABSTRACT SECURITY CLASSIFICATION Unclassified
22a. NAME OF RESPONSIBLE INDIVIDUAL James Battis	22b. TELEPHONE NUMBER (Include Area Code) (617) 861-3222 22c. OFFICE SYMBOL AFGL/LWH

CONTINUED FROM PAGE 1

CONT

Diffracted arrivals travelling around the base of the low-velocity region further constrained its depth. Other minor low-velocity zones, possibly indicating layers with increased silt content, were also indicated by the inversion model.

This study showed that cross-borehole tomography can be a useful tool in delineating velocity anomalies roughly perpendicular to paths between the boreholes, but that velocity anomalies parallel to the boreholes will be smeared unless additional constraints are imposed. A modification to the data acquisition technique to help overcome this problem would be to use additional high-energy shot-points on the surface between the boreholes.

TABLE OF CONTENTS

FIGURE LEGENDS

TOMOGRAPHIC INVESTIGATIONS AT LANDFILL 4
HILL AIR FORCE BASE, LAYTON, UTAH

1.0 INTRODUCTION

The work covered under this report was performed in accordance with SBIR contract no. F19628-84-C-0130 between Weston Geophysical Corporation and U.S. Air Force Geophysics Laboratory, Hanscom Air Force Base, Bedford, Massachusetts.

Since field seismic measurements for improvements in technology are integral parts of this Air Force contract, it is desirable to perform such activities at locations where previous investigations have taken place that provide background data. This overall procedure, combining experimental and test efforts at sites where pre-existing information can be used to usefully constrain the experimental program, results in the most cost-effective type of field development effort.

One of the locations available to Weston Geophysical for the field work segments of our SBIR R&D contract, is a location at Hill Air Force Base, Utah; at this facility, earlier geophysical measurements were utilized for evaluation of a slurry trench emplacement. Surface seismic profiling had taken place there and disclosed that part of the slurry trench installation coincided with a near-vertical variation in depths to the water table of approximately three feet. This variation from the upper, or natural ground condition, to the opposite, or "landfill" side of the slurry trench installation is characteristic of a vertical cutoff. Drillhole data concerning geologic stratigraphy is also available, and several additional holes were drilled for the insertion of testing and detection equipment.

It is significant that this seismic velocity measurement program is the first known instance of such a field evaluation of a vertically constructed feature of rather finite cross-sectional extent and in a regime of varying water table elevations.

2.0 FIELD TESTING PROGRAM

Three separate locations along the slurry trench alignment were chosen for performing the seismic field measurements and the recording of field data with the Weston-developed digital recording system, the WesComp™ [see Figure 1]. With the pre-existing data and general knowledge of geologic conditions, some of the data processing efforts and analysis developments could be constrained to the recognition of such information; namely, bedrock does not exist within the range of influence for these measurements. Also, it was understood that the slurry trench installation extended to a clay layer occurring at a depth of approximately 47 feet below ground surface. Furthermore, a slurry trench is a predictable low-velocity zone that can be anticipated as probably bounded by saturated velocity materials on either side but at different elevation levels. Field logistical complications are minimized by ready access developed in the previous on-site experience.

2.1 Data Acquisition Program

At each of three positions selected for field measurements, boreholes were drilled to the maximum depth of the slurry trench installation; a 6" cased shothole, designated by the prefix "S" in Figure 1, was placed on the upper side of the slurry trench and a 3" cased receiver hole, designated by the prefix "R", was drilled through the landfill into the lower, or downstream, side of the slurry trench. Exceptions were: at the location south of Landfill 4, an additional shothole was also drilled on the upstream side of the trench; and at the location east of Landfill 4, a deep receiver hole was not available. A non-destructive source of imaging, a sparker device, was used for generation of seismic wave energy; the source was placed at varying depths in the upstream hole of each borehole pair. Detection of seismic wave energy was performed in the downstream hole using a string of 6 velocity-sensitive geophones enclosed in an oil-filled casing. The geophone string was moved to different locations in the hole to obtain different depths of coverage. At the south location, shots were also fired in S-3 and recorded in S-2 to provide a cross-borehole path which did not pass through the slurry trench.

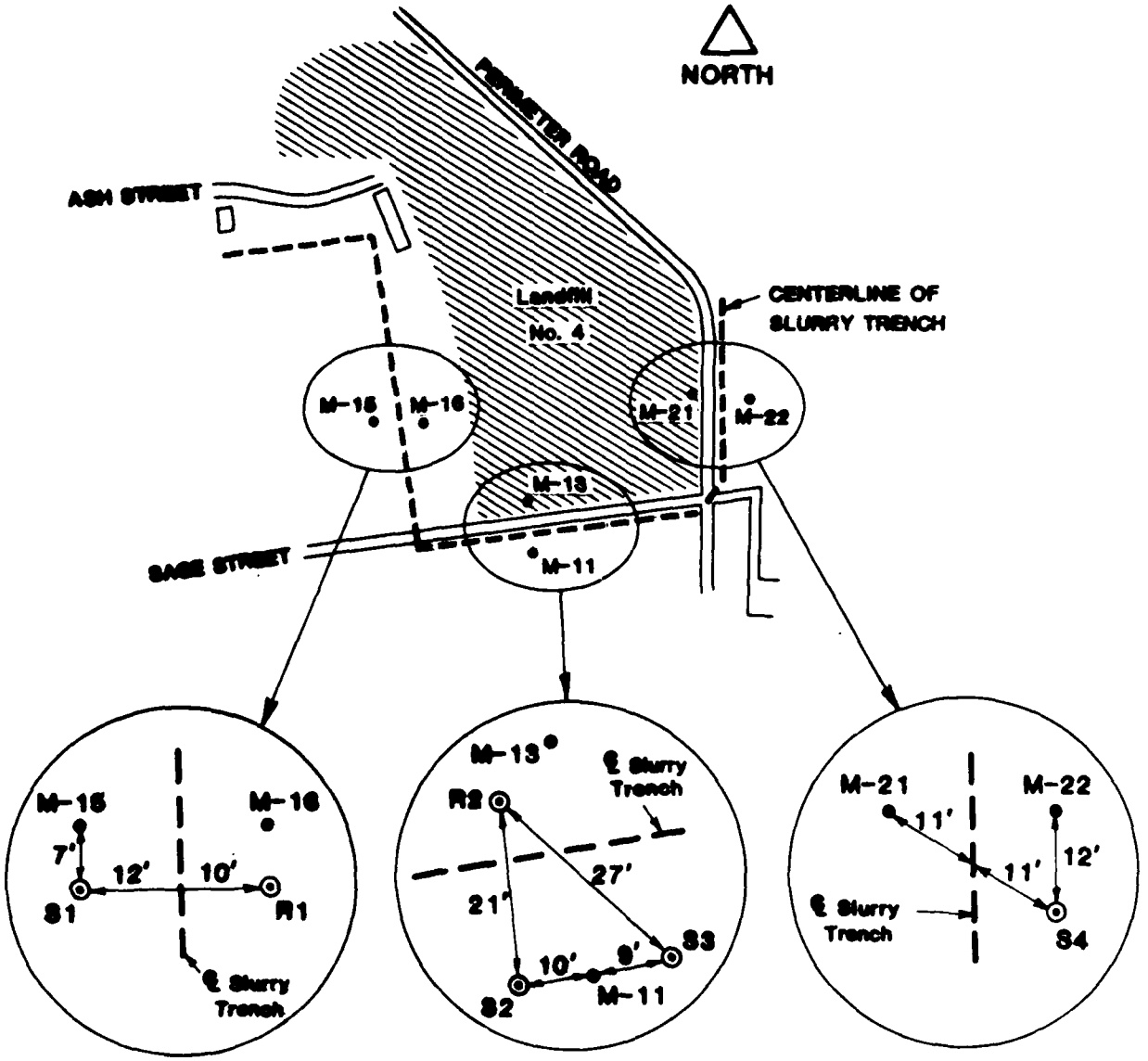

Figure 1. Location of test areas.

For this program, all seismic energy generation and detection took place below the levels of standing water in each of the boreholes. The detected seismic signals were recorded by means of Weston's WesComp™ digital recording system and a limited amount of field playback took place to assure satisfactory record quality. No modifications were required of the field seismic system for this phase of Weston's SBIR program.

2.2 Data Processing Efforts

Since large amounts of data were recorded at each of the borehole array locations, a significant part of our measurement program efforts, and an integral part of this SBIR program, was concerned with an improved and more effective data processing methodology, which is discussed further below.

3.0 DATA PROCESSING AND INTERPRETATION

3.1 Introduction

The seismic data were interpreted using a tomographic technique. The results were then displayed as cross-sectional plots of seismic velocity variations between each set of boreholes. As described further below, several difficulties were experienced in processing the data. These difficulties included: high attenuation of energy due to passage through the slurry trench and near-surface unsaturated regions; complications due to diffracted raypaths going around the bottom of the trench; apparent non-verticality of some of the boreholes; and non-optimum placing of shots and receivers. In order to overcome these problems, an iterative approach was developed involving comparison between predicted and observed characteristics of the data, and adjustment of the inversion model to improve the fit to the observations.

The final results suggest that the slurry trench affectively terminates at depths between 35 and 40 feet at the test locations south and west of Landfill 4. At the test location east of Landfill 4, termination of the

trench near 40 ft. depth is also inferred, although at this location the data resolution is poor and a greater depth for the trench cannot be excluded.

3.2 Description of Tomography Technique

Seismic tomography is based on the principle of the CAT-scan used in medicine. In medicine, sensitive detectors are used to measure the absorption of electromagnetic energy passing through various body tissues. By measuring the absorption at different angles, an image of the interior structure of the body can be built up. In seismic tomography, elastic waves are used instead of electromagnetic waves, and travel times rather than absorption are used to obtain a velocity image of the earth. However, the general inversion technique is the same in both cases. For a review, see Worthington [1984].

Figure 2 represents a vertical cross-section of the earth between two boreholes, as used in this study. Shots are fired at intervals along the left borehole and recorded using geophones down the right borehole. In Figure 2, two shots and two receivers are shown, but in general many shots and receivers are used to obtain a multiplicity of raypaths.

The analysis procedure is as follows -

1. The region between the boreholes is divided into a number of rectangular cells, within each of which the P-wave velocity is assumed to be constant. A typical cell is shown on Figure 2. An initial estimate is made for the velocity in each cell.
2. Rays are traced from each shot to each receiver, and predicted travel times computed for each path by summing the product of ray length and slowness [reciprocal of estimated velocity] in each cell along the path.
3. The predicted travel times are compared with the observed times and the cell slownesses adjusted to improve the fit between

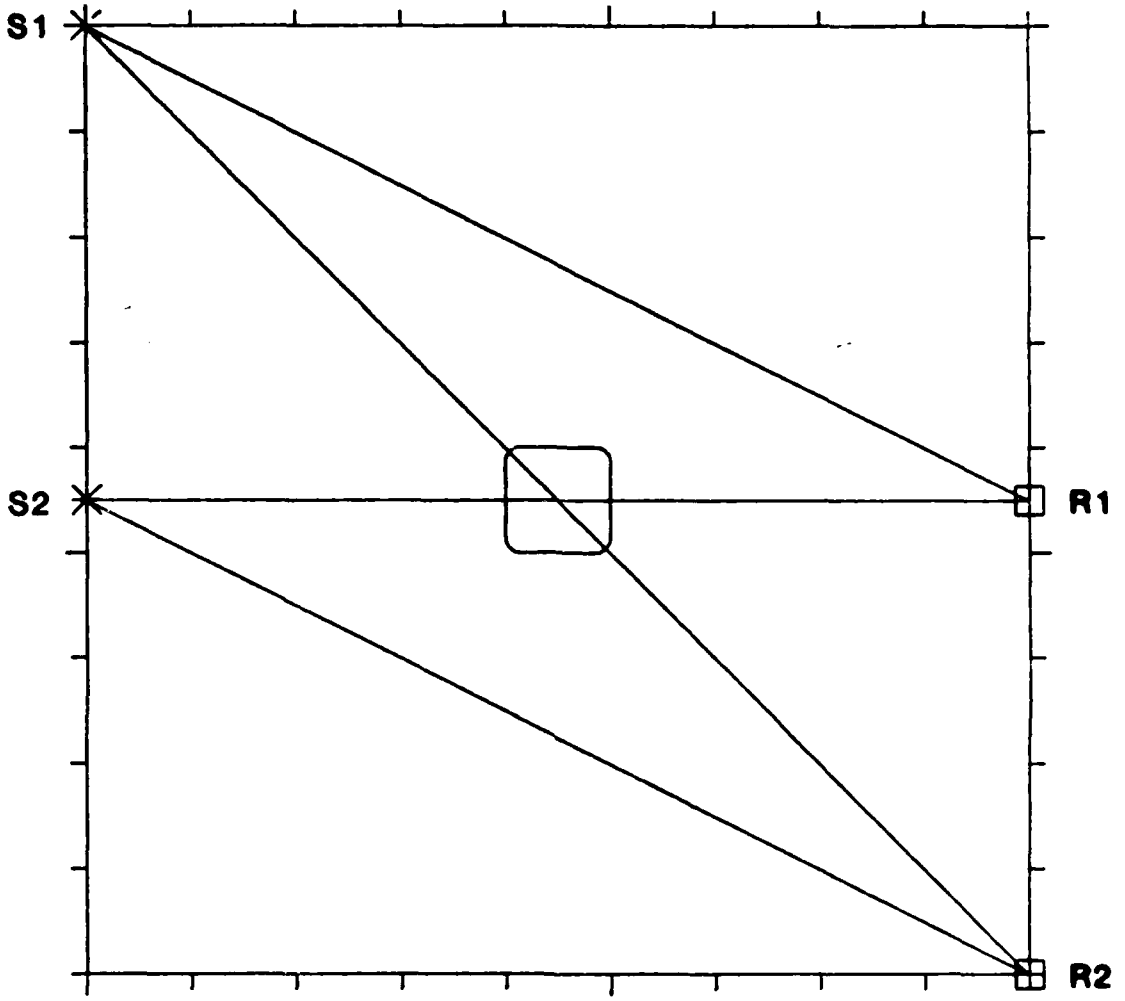

Figure 2. Simplified tomography example.

predicted and observed travel times. In Figure 2, rays S1R2 and S2R1 pass through the indicated cell and therefore can be used to update the slowness estimate in the cell.

4. This procedure is repeated as many times as necessary to obtain a satisfactory convergence.

A number of iteration schemes to improve the slowness estimates have been proposed. After trying several methods, we adopted a back-projection method in this study. Errors in the travel times are distributed back along the raypaths according to the proportion of the raypath spent in each cell. Travel time errors and ray lengths are accumulated for each cell and their ratio then used to adjust the slowness estimate in the cells.

The advantage of the back-projection method is that it is stable, is relatively insensitive to the presence of errors in the data caused, for example, by mis-picking of first breaks, and converges to a solution fairly rapidly. The disadvantage of the method is that velocity anomalies tend to be smeared out along the raypaths. This is illustrated in Figures 3 and 4.

Figure 3 shows an L-shaped velocity anomaly consisting of a 5,000 ft/sec region embedded in a uniform 3,000 ft/sec background field. Theoretical travel times were computed through the region from 10 shots to 10 receivers, then inverted using the back-projection method. Figure 4 shows the resulting inversion model.

As can be seen, the horizontal leg of the anomaly has been recovered accurately. This is because this region is well bracketed by rays, some of which pass through the anomaly, others on either side of it. This is not the case, however, for the vertical leg of the anomaly, which is therefore smeared out.

The situation could be improved by using additional shots or receivers on the top surface of the model. This was tried at the site location

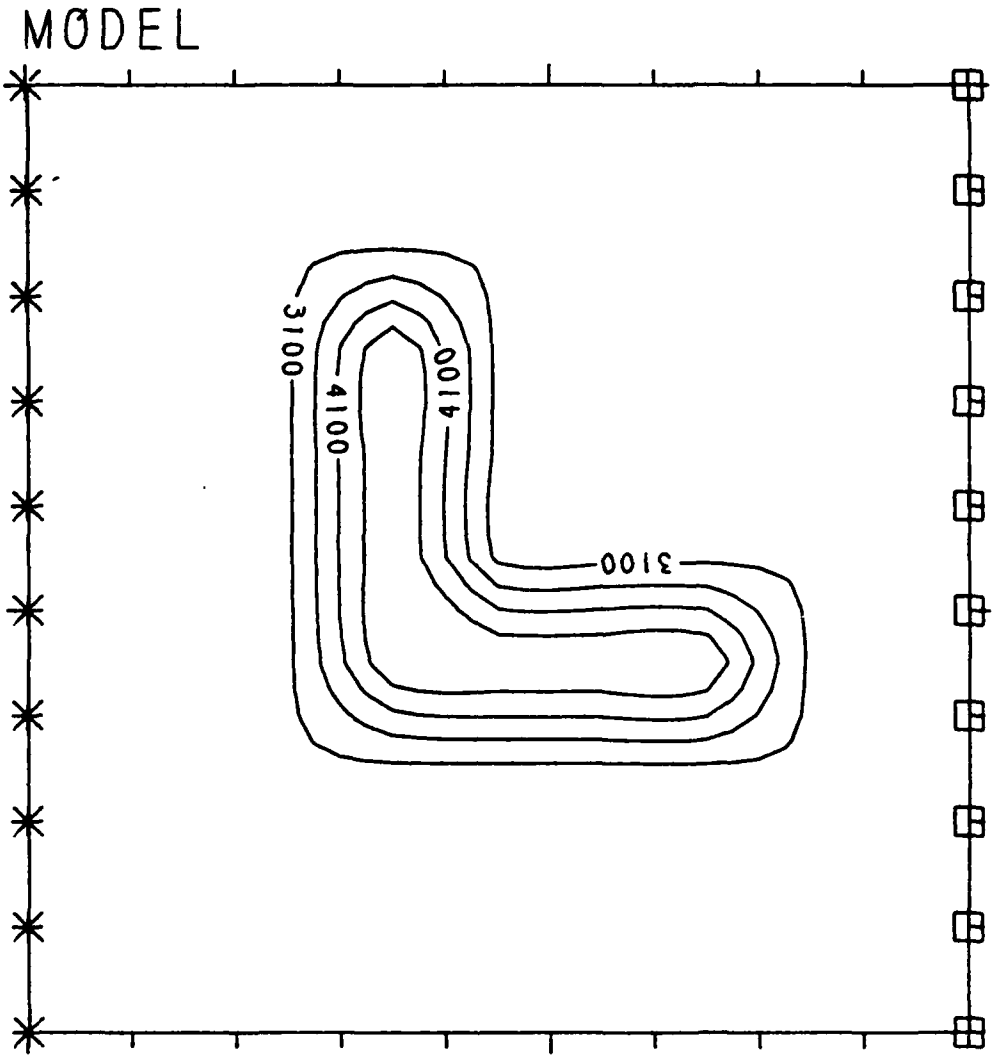

Figure 3. Test model with an 'L'-shaped velocity anomaly.

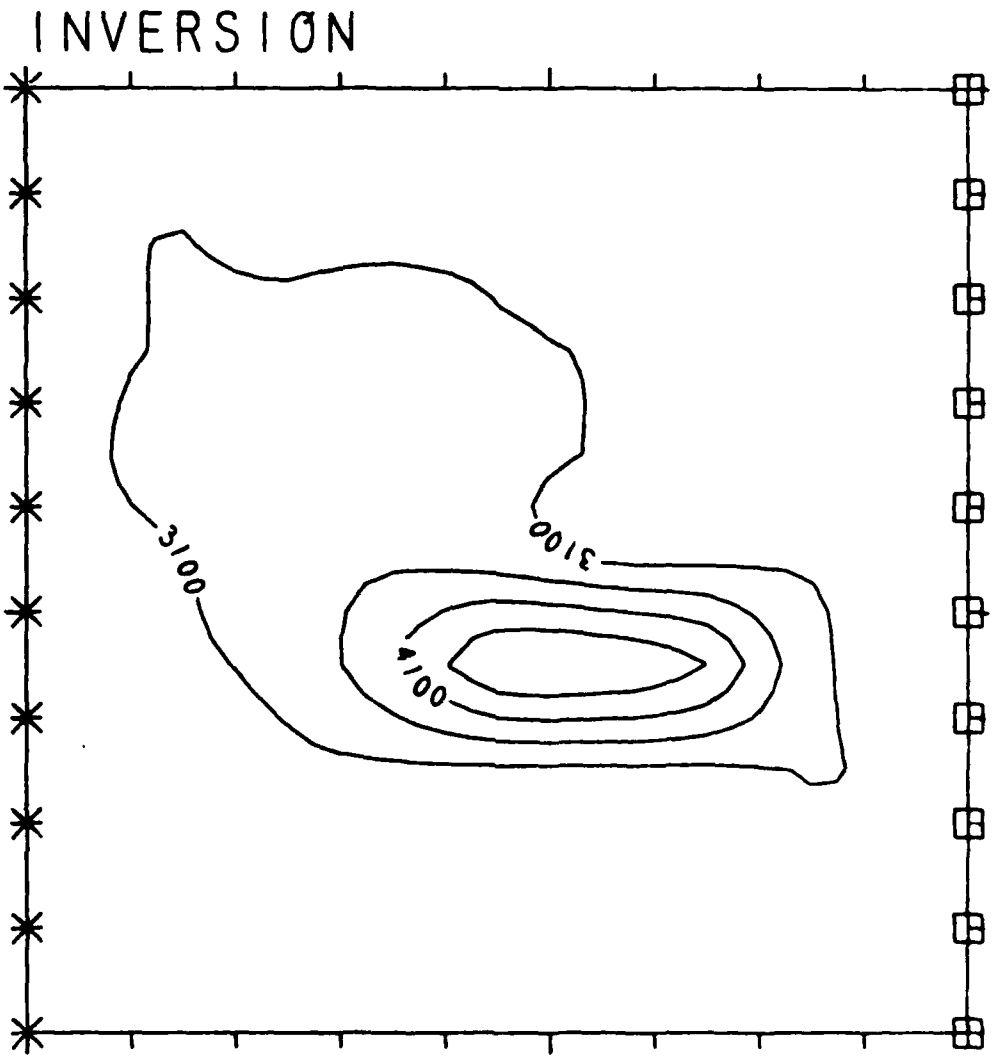

Figure 4. Tomographic inversion of test model.

east of Landfill 4, by placing additional receivers at the surface, but it was found that high absorption of energy in the unsaturated near-surface materials and surface noise severely limited the usefulness of the surface data. In retrospect, it may be better to fire additional high-energy shots at the surface, recording the energy down each borehole. In this study, in order to overcome the problem of horizontal resolution, additional constraints were therefore placed on the inversion model, as described below.

Other factors which need to be considered in the inversion process are a decrease in resolution near the upper and lower edges of the model, where few rays are present, and ray bending. Rays will be bent because of refraction at velocity boundaries; the assumption of straight rays can therefore produce artifacts in the inversion. This turned out to be a significant complication in this study, because of the large velocity contrast present between the low-velocity slurry trench and the surrounding saturated sediments.

A curved ray algorithm was therefore developed to take ray bending into account. The first iteration was performed with straight rays, but subsequent iterations used curved rays based on the velocity model from the previous iteration. Synthetic examples showed that this improved the accuracy of the resulting inversion.

3.3 Preliminary Processing

The seismic data collected in the field using Weston's WesComp™ system were offloaded to our VAX 750 system. An interactive program was used to display the data on a graphics screen for picking of first breaks. The first break times were entered into a file together with coordinate information, and this file then read by the tomography program, which is also interactive. Another program was used to trace rays through simplified models and superimpose the ray travel times on the seismic data. This was found particularly useful to refine the tomography model by identifying diffracted arrivals.

3.4 Results

The site near monitoring wells M-11 and M-13, south of Landfill 4, was used as a test case to develop an appropriate processing strategy. Three sets of borehole data were acquired; between S-2 and R-2, between S-3 and R-2, and between S-2 and S-3 [see Figure 1]. The first two sets of boreholes straddle the slurry trench, whereas S-2 and S-3 are both on the south side of the trench.

3.4.1 Boreholes S-2 and R-2

Shothole S-2 is 14 feet south of the estimated center of the slurry trench, 10 feet west of monitoring well M-11 [see Figure 1]. It is approximately 50 feet deep. Five feet is lost from the bottom of the hole because of the length of the sparker unit, so that the first shot was fired at 45 feet depth. The shallowest shot occurred at 22 feet depth. Receiver hole R-2 is 7 feet north of the slurry trench, 11 feet southwest of monitoring well M-13. Receivers were used at 2 foot intervals from 52 feet - 22 feet depth. Figure 6 shows the total distribution of shots and receivers.

First break arrivals for shots and receivers near the bottom of the hole were clear and easy to pick. It was noticed, however, that the quality of the first arrivals degraded dramatically above 36 feet depth. Figure 5 shows a zero-offset seismic record [shots and receivers at the same depth] from 22 - 44 feet depth. The depth increment is 2 feet between traces. The picked first breaks are indicated by the solid line. Notice the sharp onsets below 36 feet. Shallower than this depth, the first breaks are highly emergent and could only be picked at high gain. Obviously, something significant happens to the data at a depth of 36 feet. Since Figure 5 represents shots and receivers at gradually increasing levels down the hole, the decrease in travel times down to a depth of 36 feet also implies a corresponding increase in the average velocity between the boreholes.

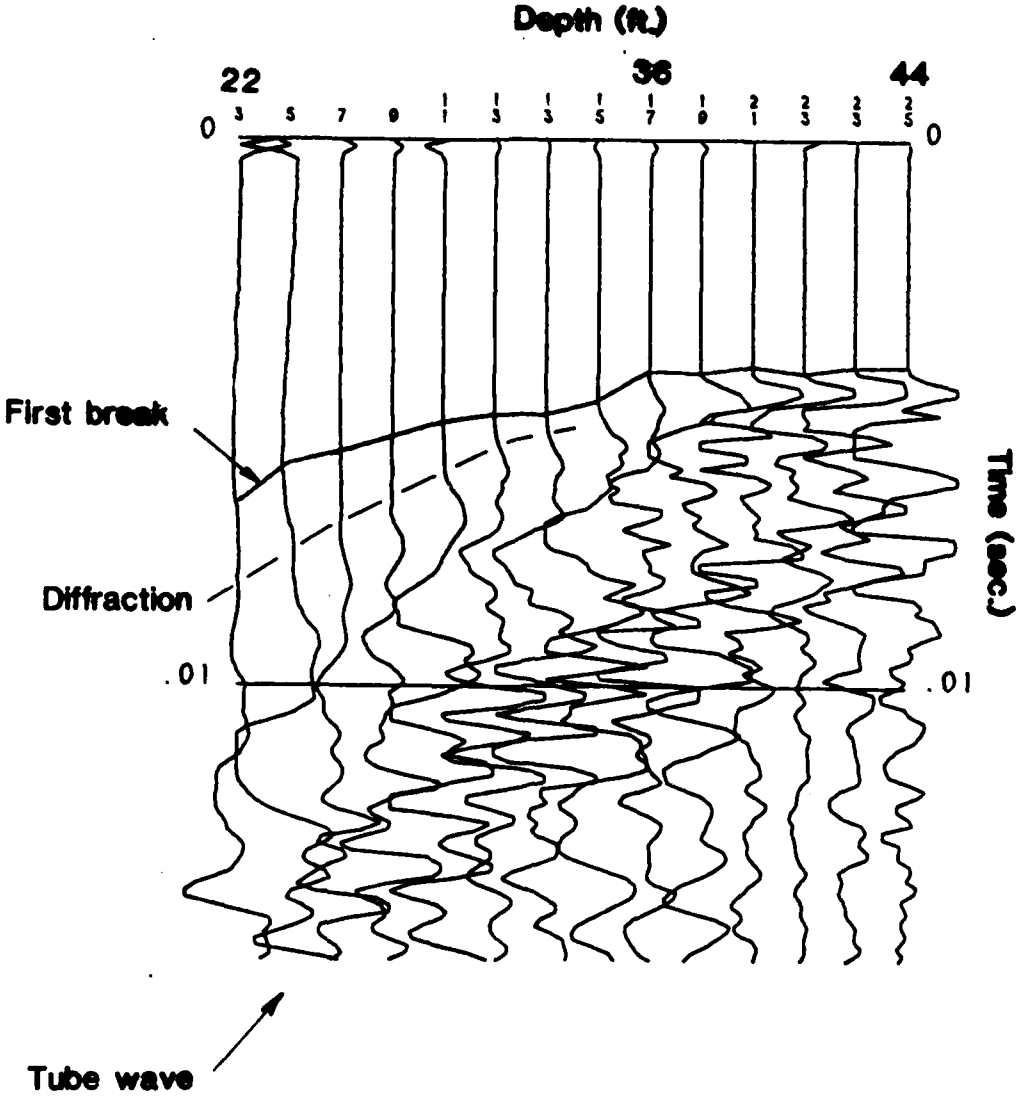

Figure 5. Seismic data recorded in borehole R-2 from shot in S-2. Sources and receivers are at the same depth.

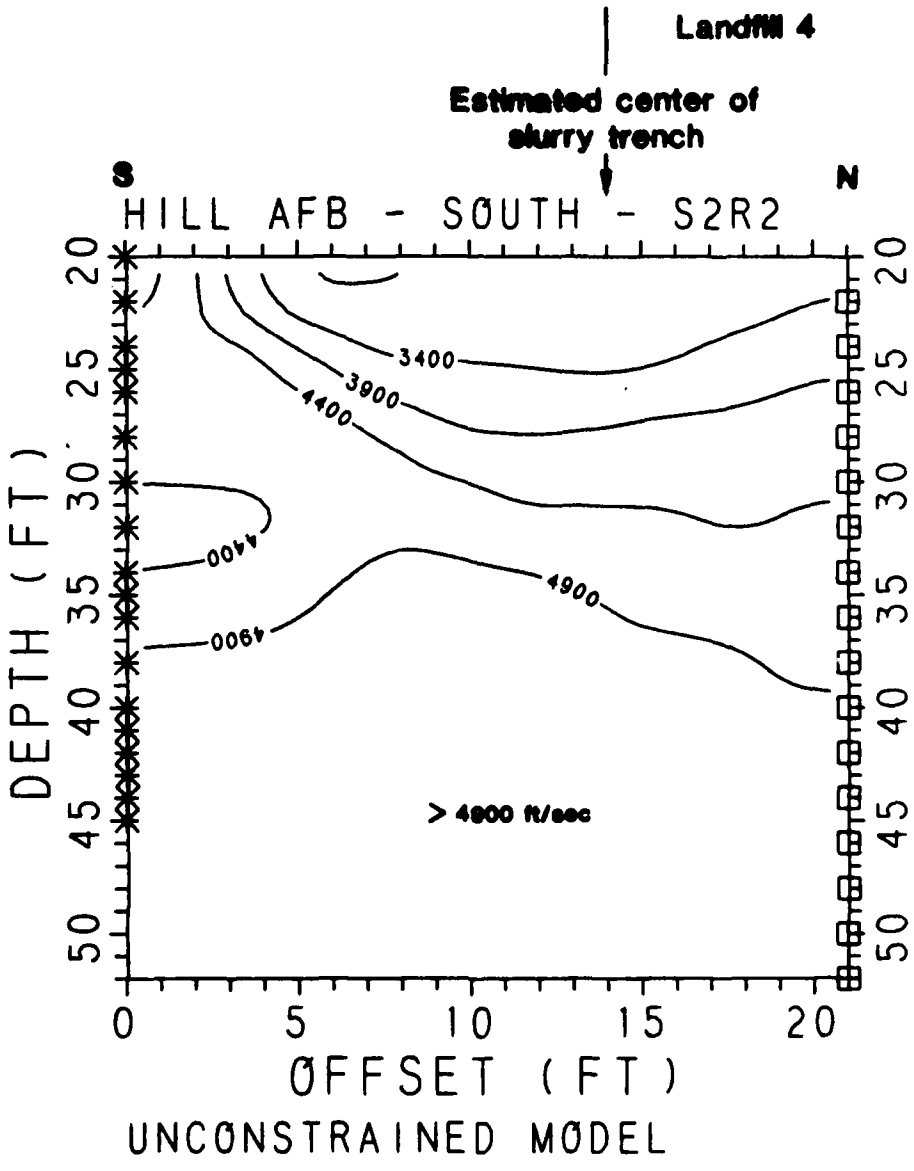

Figure 6. Unconstrained tomographic inversion. Boreholes S-2/R-2.

Figure 5 also shows other coherent arrivals. A high frequency tube wave is present, which is a water wave travelling up the receiver hole. There is also a low frequency arrival occurring just after the first break arrival, which appears to intersect the first breaks at the point where they lose amplitude. This arrival is now believed to represent a diffraction around the base of the slurry trench [see discussion below].

The first break times were inverted using the tomography algorithm to produce a map of P-wave velocity variations between the boreholes, starting with a uniform velocity field. The region was subdivided into 10 cells horizontally and vertically, giving 100 cells in all. Trials with fewer and larger numbers of cells showed that 100 cells was about the optimum for adequate resolution and speed of inversion. A curved ray procedure was used, but was found to produce only minor differences from a straight ray inversion. Figure 6 gives the results displayed as velocity contours at 500 ft/sec intervals.

Upon first examination, Figure 6 appears reasonable. The picture is one of a primarily horizontally-layered medium with velocity increasing downwards. Upon further examination, however, problems with this model emerge.

The main problem is the presence of 3,000 - 4,500 feet/sec material from 20 - 35 feet depth. These velocities are uncharacteristic of the unconsolidated sediments present at the site. Typically, poorly - consolidated sands, gravels and silts, which comprise the bulk of the borehole samples, would be expected to have P-wave velocities ranging from 1,000 - 2,000 ft/sec in their unsaturated state; 4,800 - 5,200 ft/sec when fully saturated. The transition in velocities also occurs very rapidly, within the last 2 percent of saturation, so that the presence of large volumes of material with intermediate velocities caused by near saturation is unlikely. Uncompacted clays fall into the same general velocity range. Velocity values of 3,000 - 4,500 ft/sec are more typical of partially-cemented sediments, dense glacial tills, or weathered bedrock, none of which are inferred to be present at these

shallow depths at the site. Another difficulty is that the 4,900 ft/sec contour, which would be interpreted as the water table, occurs at 35 feet depth. Yet standing water is present in monitoring wells M-11 and M-13 shallower than 25 feet.

There are two possible explanations for the discrepancy. The first is that the velocities of 3,000 - 4,500 ft/sec are caused by errors in picking first breaks. Over 21 feet, however, a picking error of 1.5 millisec [msec] would be required to reduce a 5,000 ft/sec velocity to 3,500 ft/sec. While first breaks are difficult to pick above 35 feet depth, the maximum picking error is estimated to be several samples, or .25 - .3 msec, at most, so this does not appear to be a likely explanation.

A more reasonable solution is that the intermediate velocities are due to velocity smearing in the tomography inversion. Assuming that the slurry trench is present between S-2 and R-2, it is likely to have a velocity of 1,000 ft/sec or so, because of the entrapment of air bubbles during its formation and also because of unsaturated conditions due to its bentonite content. A 2 foot thick region of 1,000 ft/sec material, combined with 19 feet of 5,000 ft/sec material, would give an average velocity of 3,600 ft/sec, about what is observed.

To substantiate this conclusion, the data shot between S-3 and S-2, on the south side of the slurry trench, were examined. The first breaks in this case were fairly clear at all depths and picking mostly unambiguous. Figure 7 shows the results of the inversion, displayed as patterns separating material with velocities greater than and less than 4,800 ft/sec. The inversion indicates a uniform saturated condition from 20 - 48 feet depth, with the exception of two regions of lower velocity intersecting borehole S-2 at 23 - 25 feet and 30 - 35 feet. The upper region may be an artifact of the inversion, since it is constrained by relatively few rays. The lower region, however, appears to be a real feature, and also shows up on Figure 6. The most likely explanation for this feature, if real, is that it represents increasing

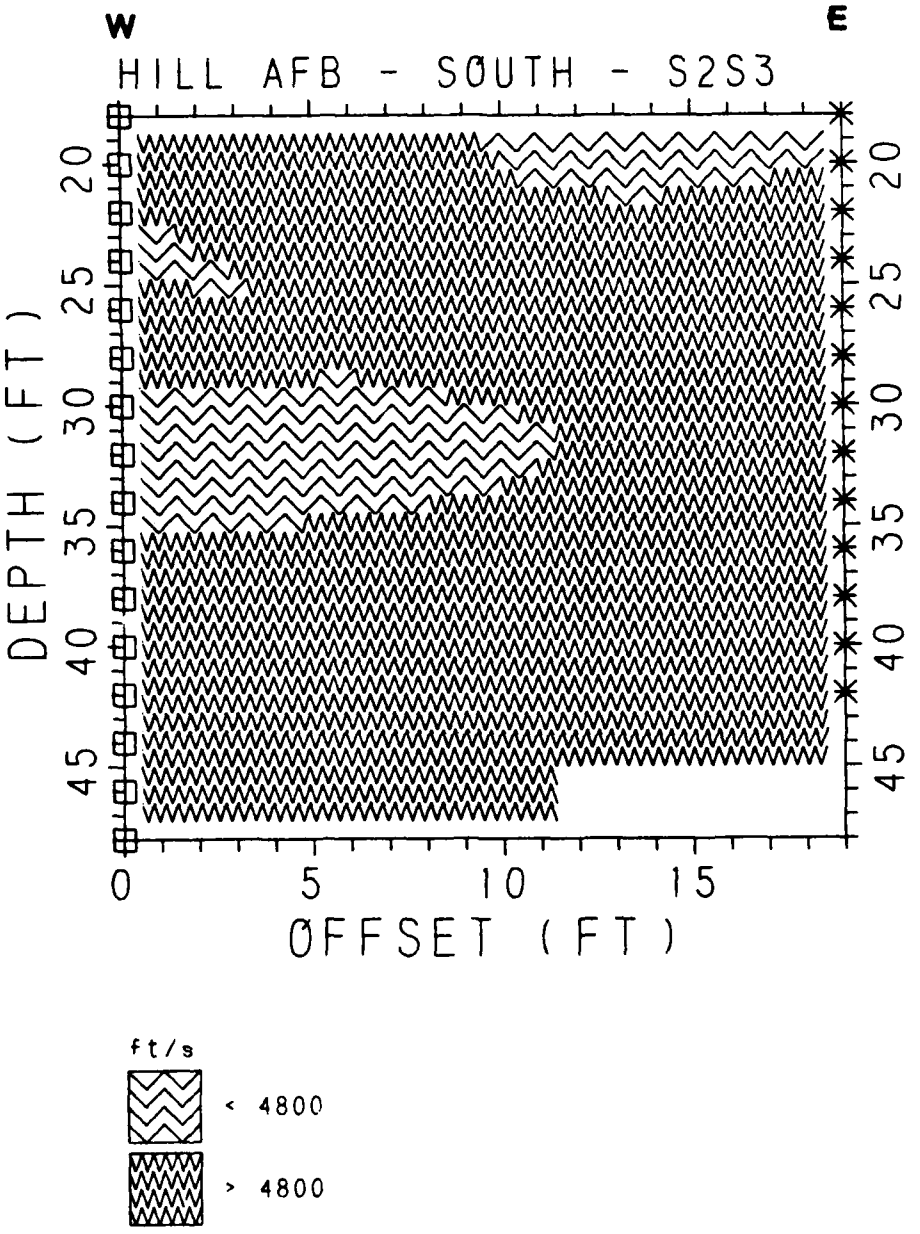

Figure 7. Tomography results south of slurry trench between boreholes S-2 and S-3.

proportions of silt, saturated but with a slightly lower velocity because of adsorbed air remaining from the time of deposition. The presence of undersaturated clay is another possibility, but considered less likely in view of the fact that clays in this area were formed in a lacustrine environment and are therefore probably fully saturated.

With the information provided by Figure 7, it is therefore clear that velocity smearing is the most likely cause of the abnormal velocities in Figure 6. Since all the raypaths travel through the slurry trench, the tomography program is unable to isolate the trench as a separate entity without additional constraints.

The next step was therefore to try the inversion by initially specifying the presence of the trench in some way. The way this was done was to start with a uniform 5,000 ft/sec velocity field throughout the region between boreholes S-2 and R-2 and to hold the velocities constant during the first iteration except in a single column at the inferred location of the slurry trench, i.e. in a column 2.1 feet thick centered near 14 feet offset from S-2. Following this first constrained iteration, the constraints were released and the inversion proceeded using the curved ray algorithm as before. Figure 8 shows the resulting inversion model.

At the location of the slurry trench, a low velocity region is now present from 20 feet to approximately 37 feet depth. Outside the trench, the 4,900 ft/sec contour lies at about 25 feet depth, in agreement with the observation of water at this depth in monitoring wells M-11 and M-13. The low velocity region intersecting borehole S-2 at 30 - 35 feet is again present and an additional low-velocity region extends from the slurry trench to intersect borehole R-2 at 35 - 40 feet depth. As shown in Figure 12, this low-velocity region is apparently an artifact of ray bending around the base of the slurry trench and is not real. Figure 9 redisplays these features as patterns separating material velocities greater than and less than 4,900 ft/sec.

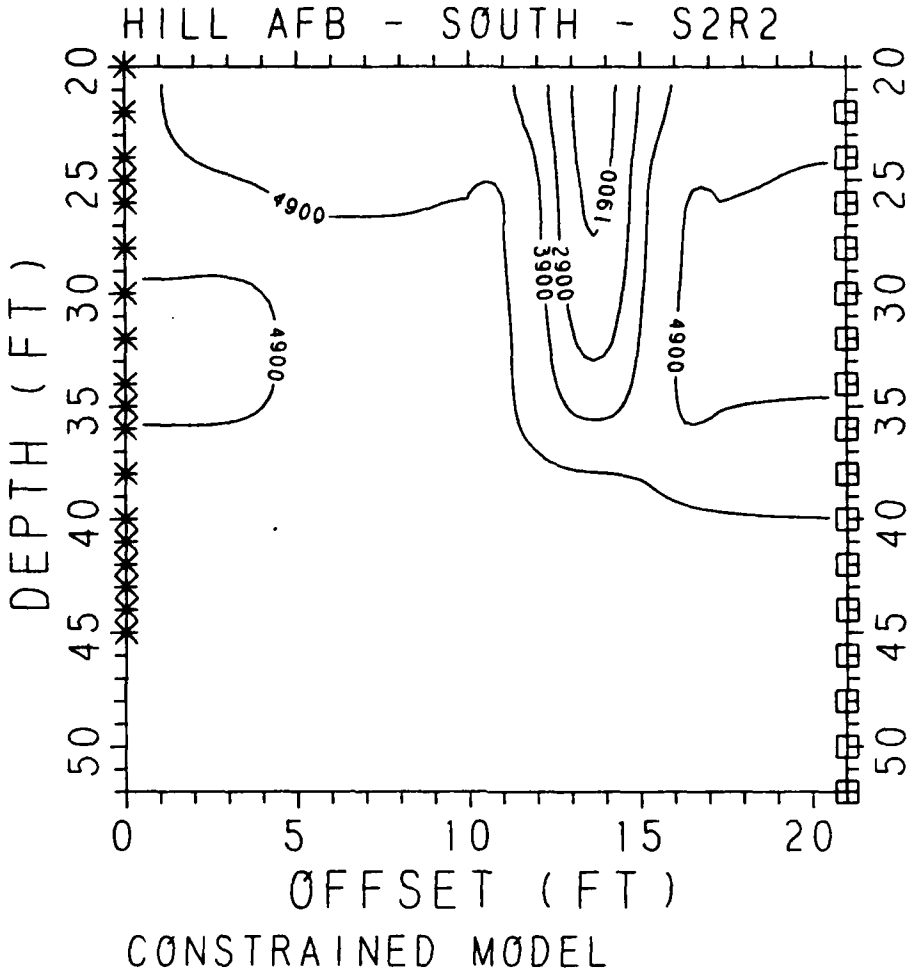

Figure 8. Constrained tomographic inversion through slurry trench. South location.

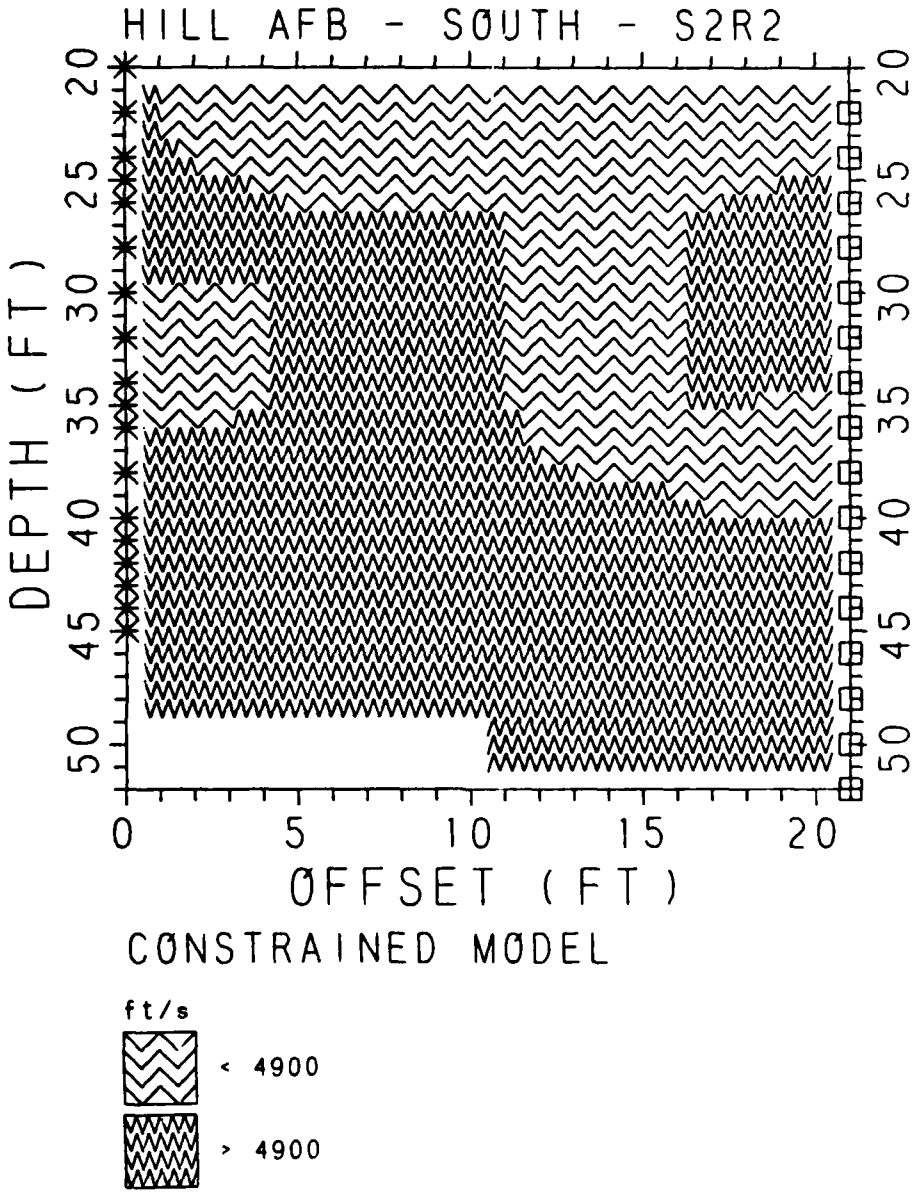

Figure 9. Results of Figure 8 displayed as patterns separating material with P-wave velocity of 4900 ft/sec.

The interpretation of Figures 8 and 9 is that the unsaturated depth of the slurry trench affectively terminates near 37 feet depth. The trench may still be present below this depth but, if so, it is saturated and undistinguishable from the material surrounding it on the basis of seismic velocities alone. Remember that the initial velocity assumed for the slurry trench was 5,000 ft/sec from top to bottom. This velocity apparently is consistent with the observed travel times deeper than 37 feet, but a much lower velocity is required at the trench to match the travel times shallower than this depth.

The next step in the interpretation was to examine the effect of the low-velocity trench upon the raypaths. Figure 10 shows the raypaths used in the final iteration. It can be seen that the rays are severely bent around the effective base of the slurry trench. This is because the first-arriving rays seek a minimum time path, which involves going around the low-velocity trench region instead of through it if at all possible.

At this point the question of possible diffractions around the base of the trench arose. Diffractions occur at sharp changes in velocity structure and would not be handled properly by the ray tracing algorithm since they do not obey Snell's Law. In general this is not a problem, since diffractions are rarely first arrivals. In the case of Figure 10, however, they provide a valid path along the base of the trench which might be quicker than the predicted raypaths. This would particularly be the case for shots and receivers just above 37 feet. If diffractions are being interpreted as first arrivals, then the trench could be deeper than indicated. Calculations indicated that the additional depth might be as much as 5 feet.

To examine this possibility, we went back to the seismic data to look for evidence of diffracted arrivals. A ray tracing program designed to compute reflected paths through simple layered models was used to simulate the effect of diffracted arrivals at different depths. The

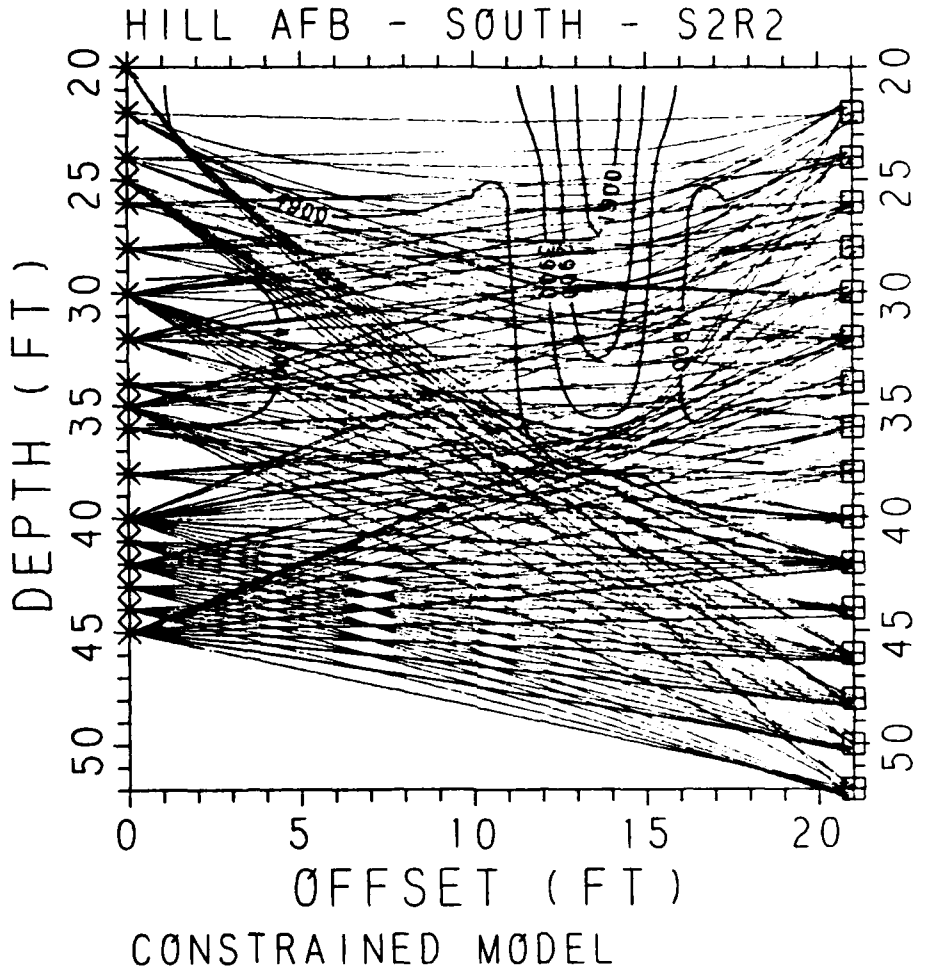

Figure 10. Curved raypaths through Figure 8 model.

results are shown in Figure 11. The left hand side of the figure shows direct and simulated diffracted arrivals for the zero-offset gather shown previously in Figure 5. The right hand side of the figure shows the seismic data corresponding to these shots and receivers, on which has been superimposed the direct and diffracted travel times for a uniform velocity of 5,000 ft/sec and a diffraction depth of 39 feet. Because a horizontal boundary was used to simulate the diffractions, the diffraction point is mid-way between the shots and receivers, rather than offset towards the receiver hole, as is the case with the slurry trench. Tests with inclined layers showed, however, that this has a negligible effect upon the results.

The diffracted travel times agree well with the onset of the low frequency event previously noted. The figure also shows, however, that the diffracted arrivals coincide with the picked first arrivals between depths of 32 feet and 40 feet. In this depth range, therefore, it appears that diffractions around the base of the slurry trench are faster than direct arrivals passing through the trench.

The diffractions constrain the depth of the trench quite tightly. Depths between 38 feet and 40 feet also give a reasonable fit to the diffractions, but this is about the maximum latitude consistent with the data. The fact that the figure of 39 feet inferred for the depth of the unsaturated portion of the slurry trench on the basis of the diffractions is not much greater than the value of 37 feet obtained using first breaks is attributed to the presence of many non-diffracted raypaths traversing the trench region [see Figure 10].

The final stage in the interpretation of the data from boreholes S-2 and R-2 was to investigate the validity of the low velocity regions shown in Figure 9. A new starting model was therefore specified on the basis of the previous results. This model consisted of a 1,000 ft/sec zone, two feet thick, extending from 20 feet to 40 feet depth at the slurry trench location, and a uniform 5,000 ft/sec velocity elsewhere. Curved rays were traced through this model and held fixed during the inversion.

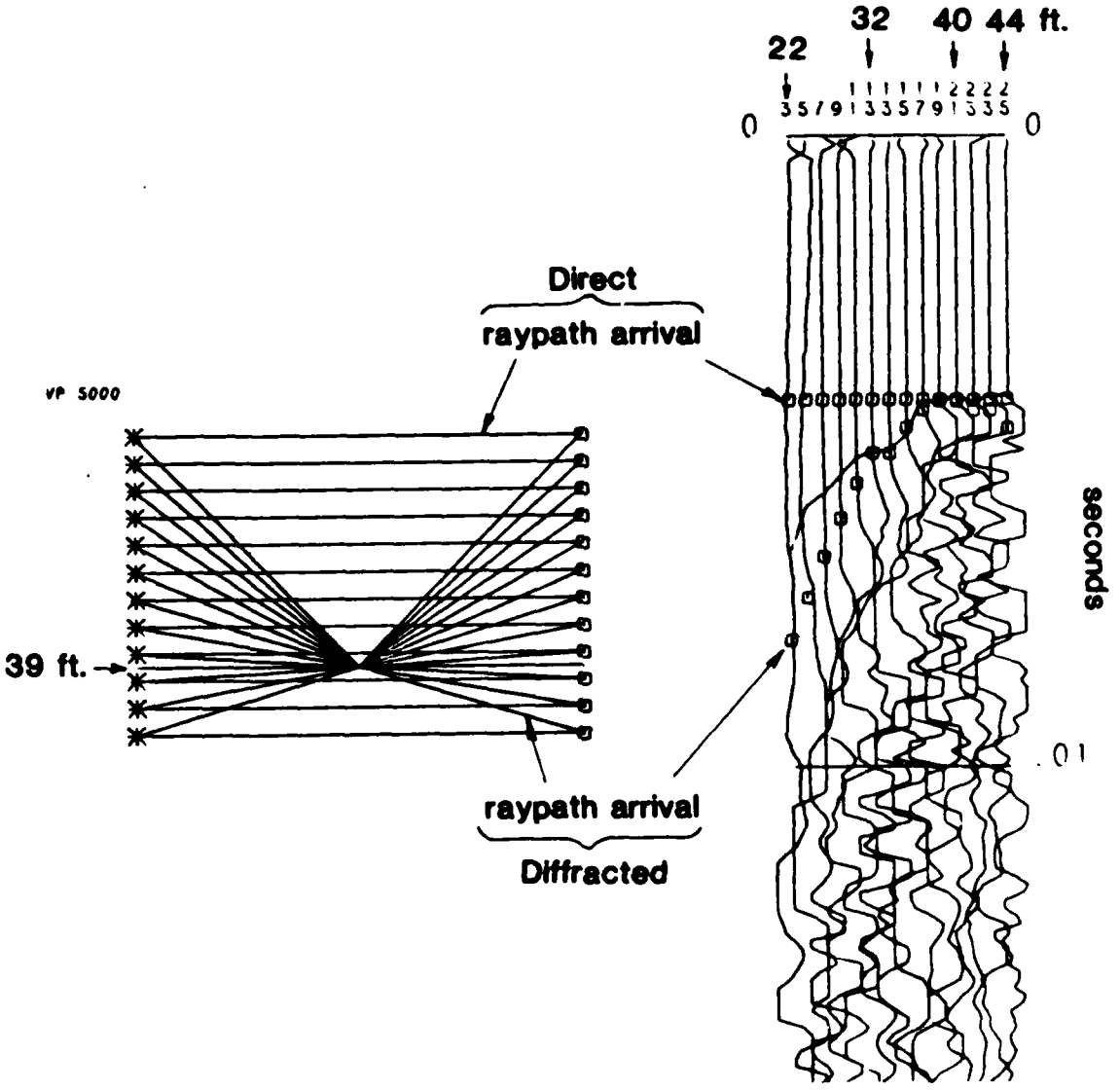

Figure 11. Raytracing to identify diffracted arrivals.

Figure 12 shows the results of the inversion. The low-velocity layer intersecting borehole S-2 is again present, and is therefore probably real, whereas the low-velocity zone previously found to the right of the slurry trench is absent, suggesting that this was an artifact of the previous model.

The data analysis and interpretation procedure for boreholes S-2 and R-2 has been described in detail to illustrate that a combination of forward modelling and the application of reasonable constraints can greatly improve the tomographic inversion process. The lessons learned from these boreholes were then applied at the other locations.

3.4.2 Boreholes S-3 and R-2

These boreholes comprise the final set south of Landfill 4. Borehole S-3 is 9 feet east of monitoring well M-11 and 19 feet southeast of the estimated center of the slurry trench. The distance measured between S-3 and R-2 on the surface was 27 feet. However, it was discovered during the inversion that this gave unreasonably high velocities [> 5,200 ft/sec] below a depth of 40 feet. A borehole separation of 26 feet gave better results and was subsequently used. Borehole S-3 may therefore be slightly out of vertical. Similar adjustments to the borehole separation were also found necessary at S-1/R-1 and S-4/M-21.

A constrained tomographic inversion was run on the first break picks as in the previous example, by adjusting only the velocities in the trench region during the first iteration, then subsequently allowing the velocities in all of the cells to adjust. In this case, the region was divided into 12 cells horizontally and 10 vertically.

The inversion results are shown in Figure 13. The effective depth of the slurry trench is inferred to be approximately 34 feet at this location. This value is supported by the diffracted arrivals [see Figure 14], which fit the first break data over the depth range 22 - 36 feet, assuming a diffraction depth at 35 feet. The reason why the

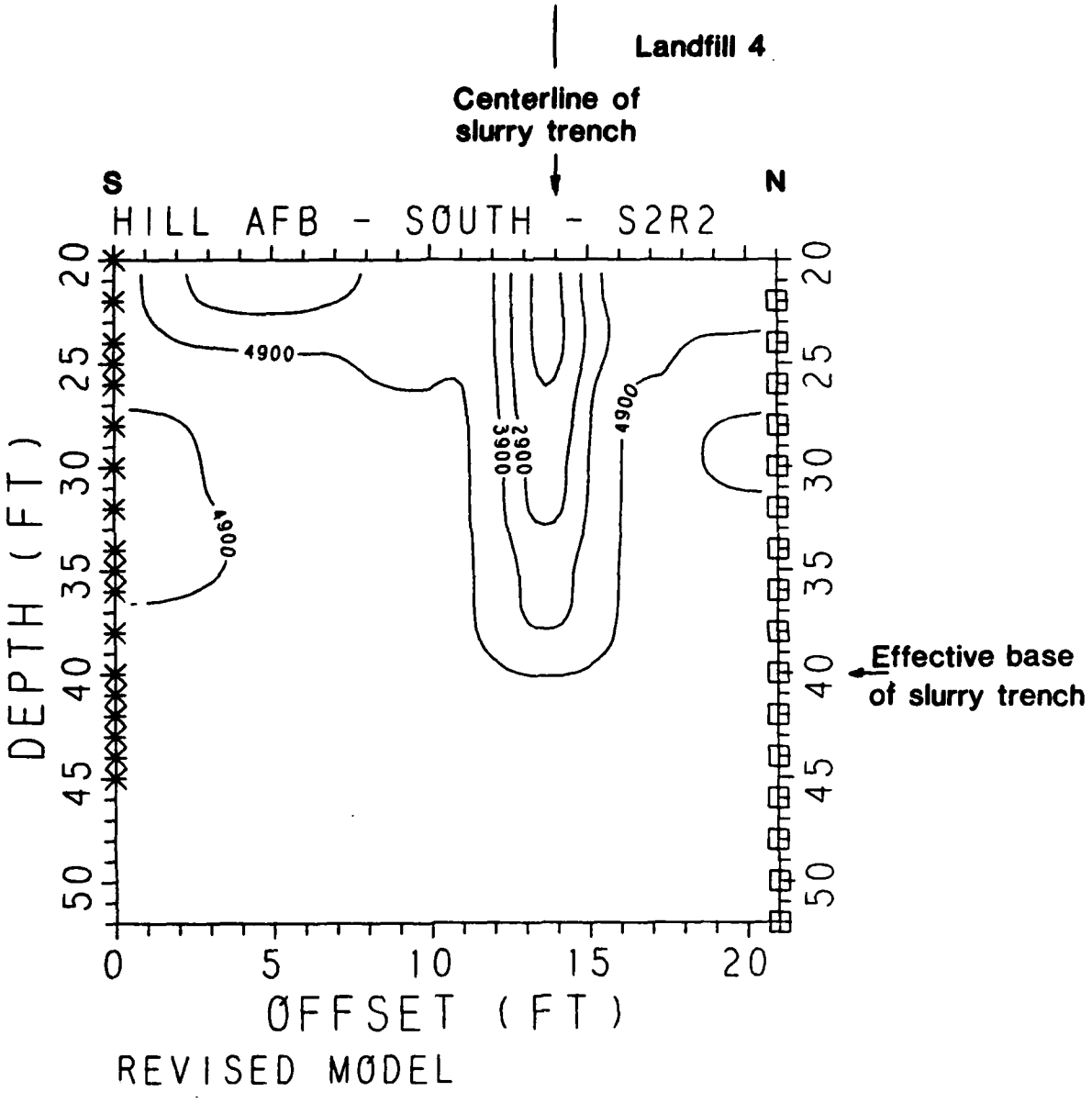

Figure 12. Final model across slurry trench between boreholes S-2 and R-2.

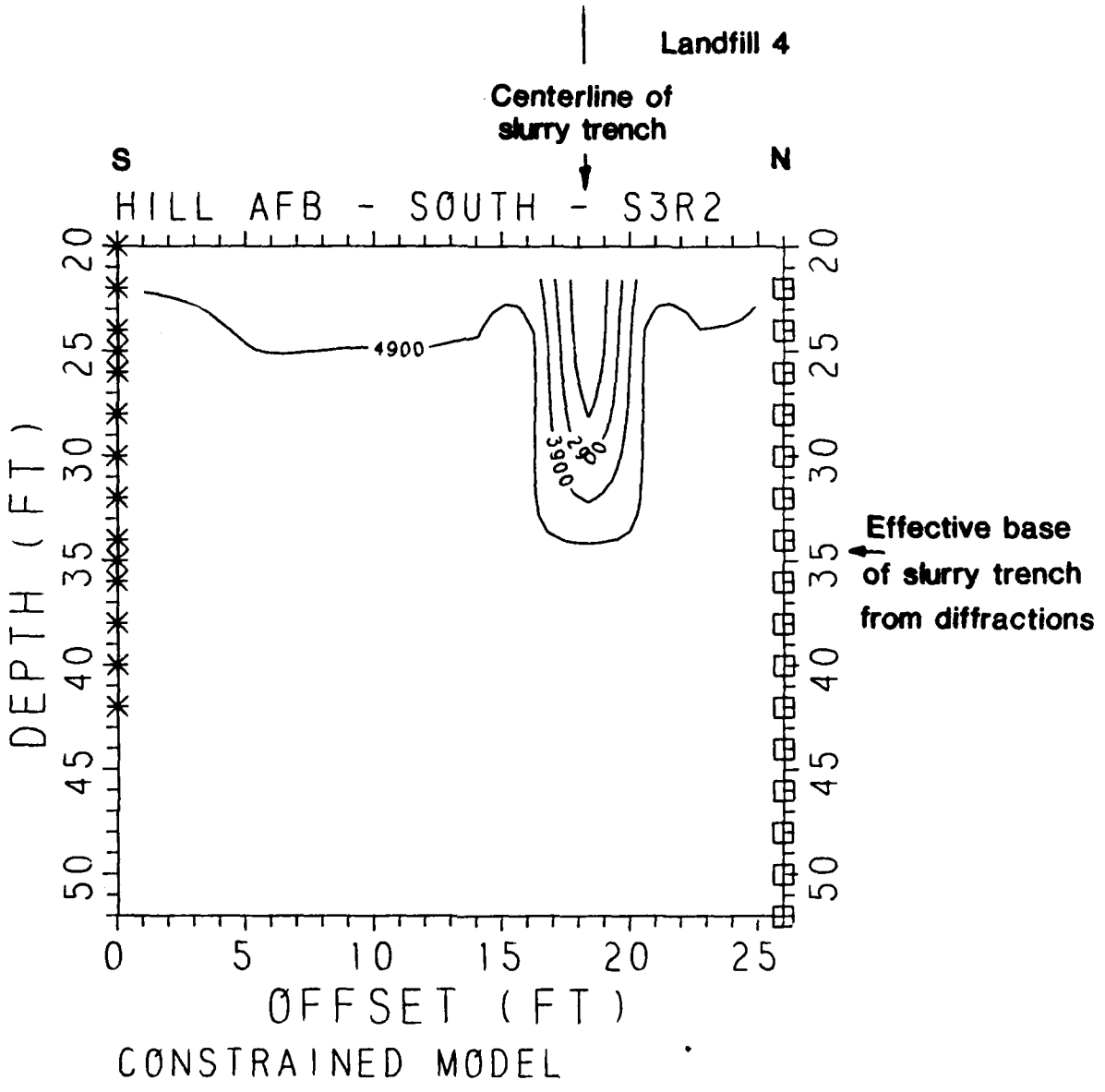

Figure 13. Constrained inversion model. Boreholes S-3/R-2.

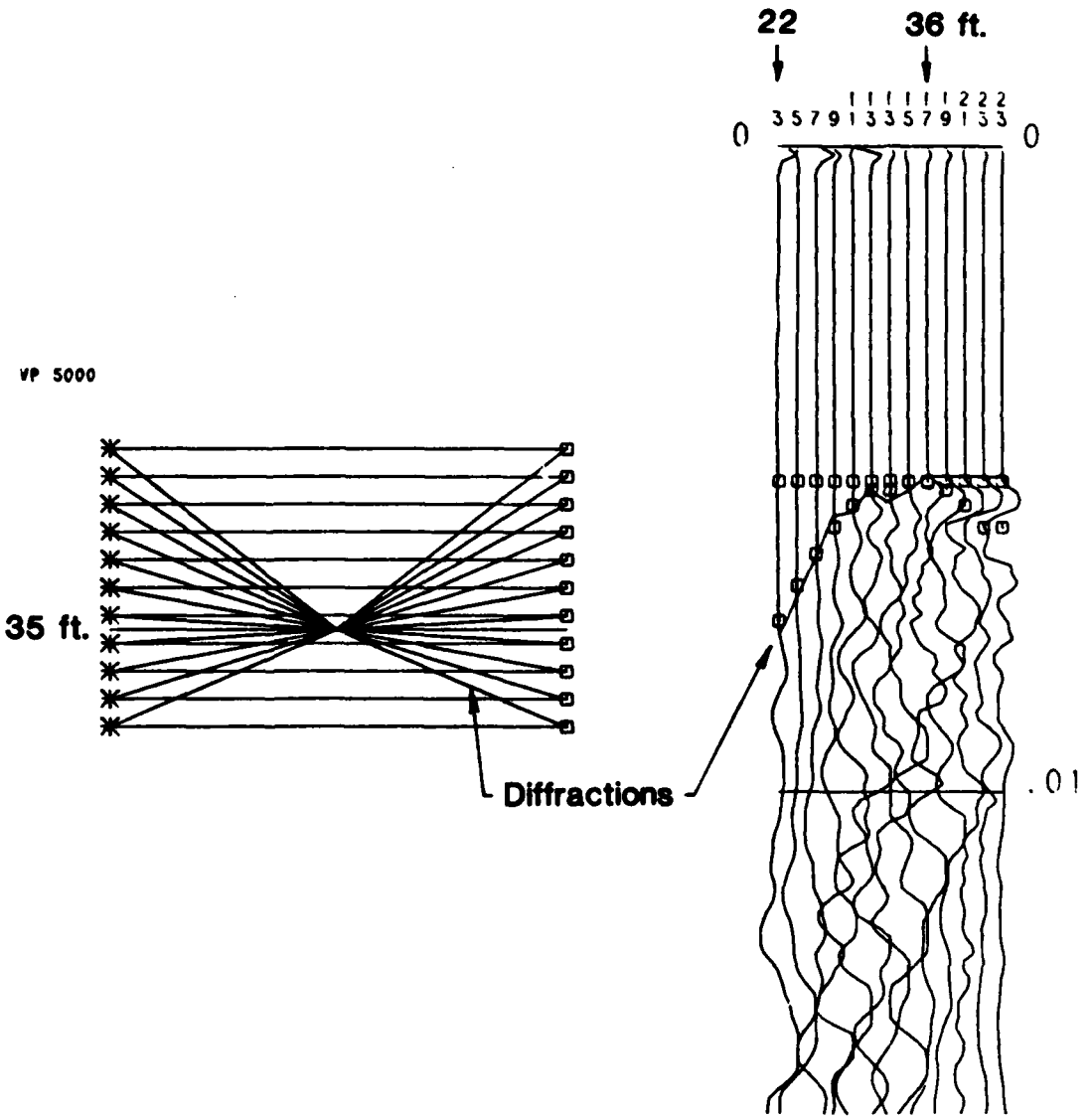

Figure 14. Diffracted arrivals between S-3 and R-2.

diffractions are observed as first breaks to a shallower depth than for boreholes S-2/R-2 can be attributed to the smaller depth of the trench and the greater distance between the boreholes.

We therefore conclude that the effective depth of the slurry trench between boreholes S-3 and R-2 is near 35 feet. Note from Figure 1 that the trench location in Figure 13 is only 5 feet east of the trench location shown in Figure 12, where the trench is inferred to be 40 feet deep. The base of the trench therefore appears to fluctuate over short distances.

3.4.3 Boreholes S-1 and R-1

These boreholes are on the west side of Landfill 4. Borehole S-1 is 7 feet south of monitoring well M-15, 12 feet west of the slurry trench. Borehole R-1 is 7 feet south of monitoring well M-16, 10 feet east of the trench. Both holes are approximately 50 feet deep. The measured distance between S-1 and R-1 is 22 feet, but it was found that a borehole separation at 21 feet was required to give reasonable velocities below 35 feet depth.

Figure 15 displays the constrained inversion model. It shows the trench terminating near a depth of 38 feet, which is increased to 40 feet when diffractions are considered [Figure 16]. Figure 15 also indicates a low-velocity zone to the east of the slurry trench above 30 feet depth, and another low-velocity zone intersecting borehole S-1 from 32 - 38 feet. To investigate whether these low-velocity zones were artifacts of the inversion related to the slurry trench, a revised model was run [Figure 17]. A 1,000 ft/sec region extending from 15 feet to 40 feet depth was placed at the location of the slurry trench and a velocity of 5,000 ft/sec assumed elsewhere. Curved rays were traced through this model and the inversion performed with these rays held fixed. The results in Figure 17 show the low-velocity zones still present but reduced in size. They may therefore be considered real.

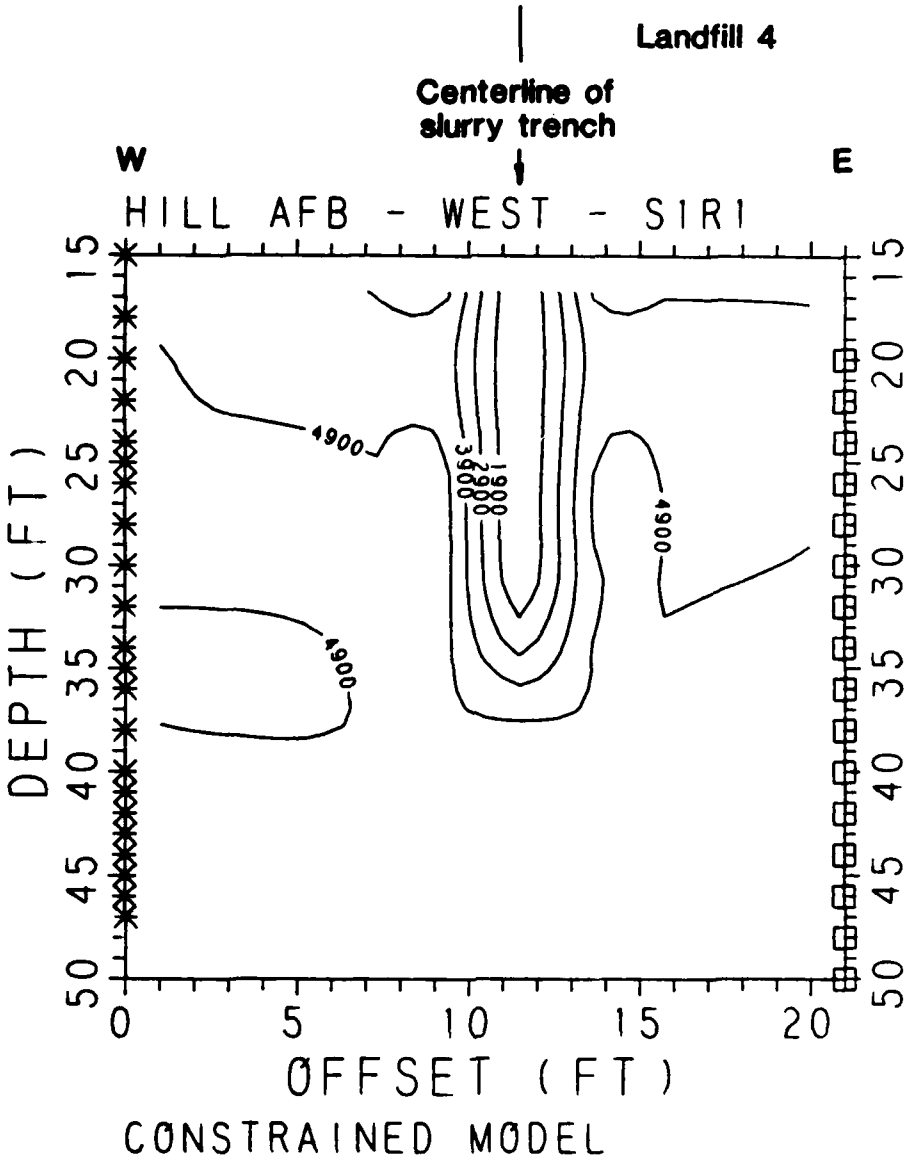

Figure 15. Constrained inversion model through slurry trench, west location.

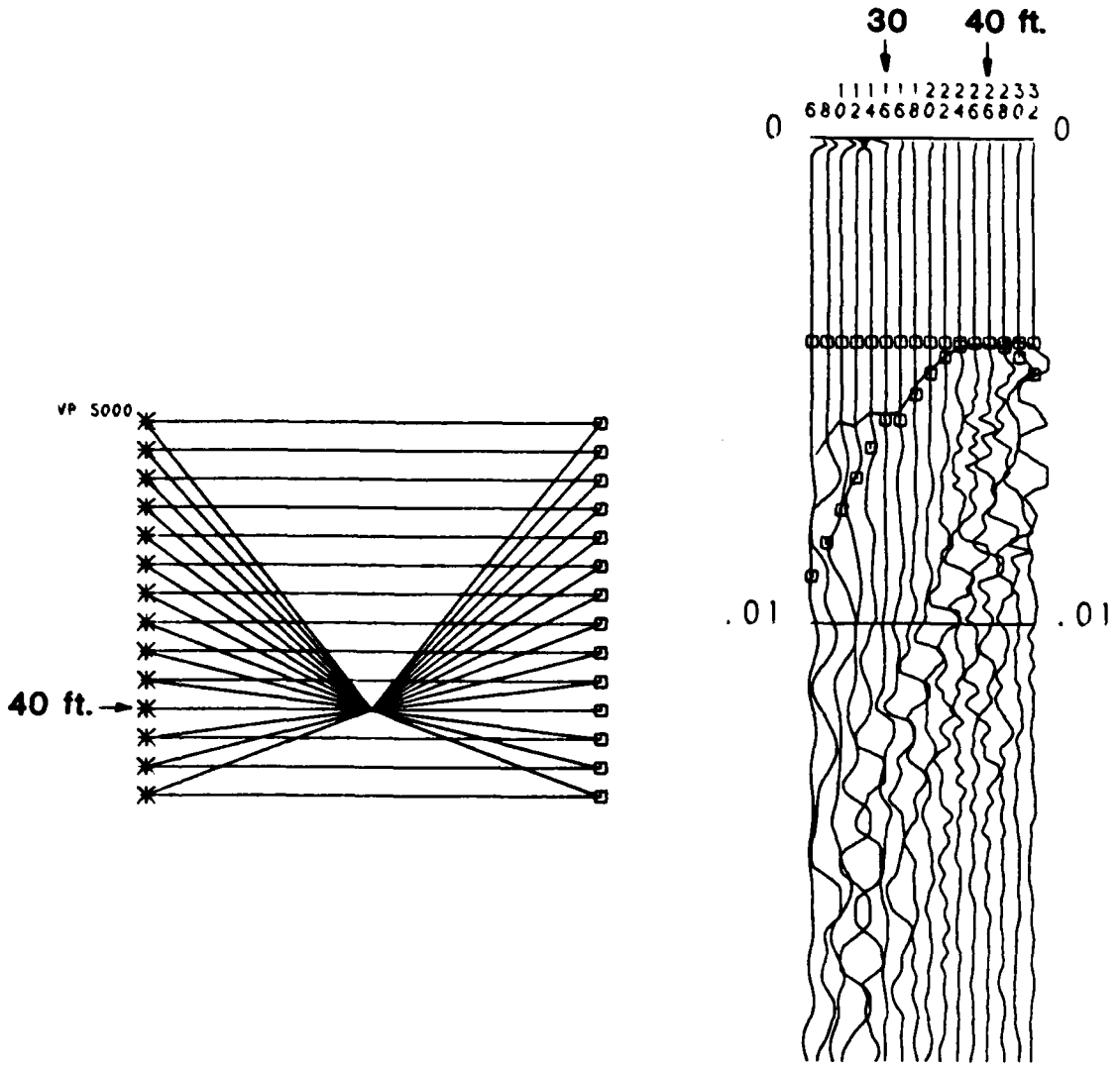

Figure 16. Raytracing to identify diffractions. Boreholes S-1/R-1.

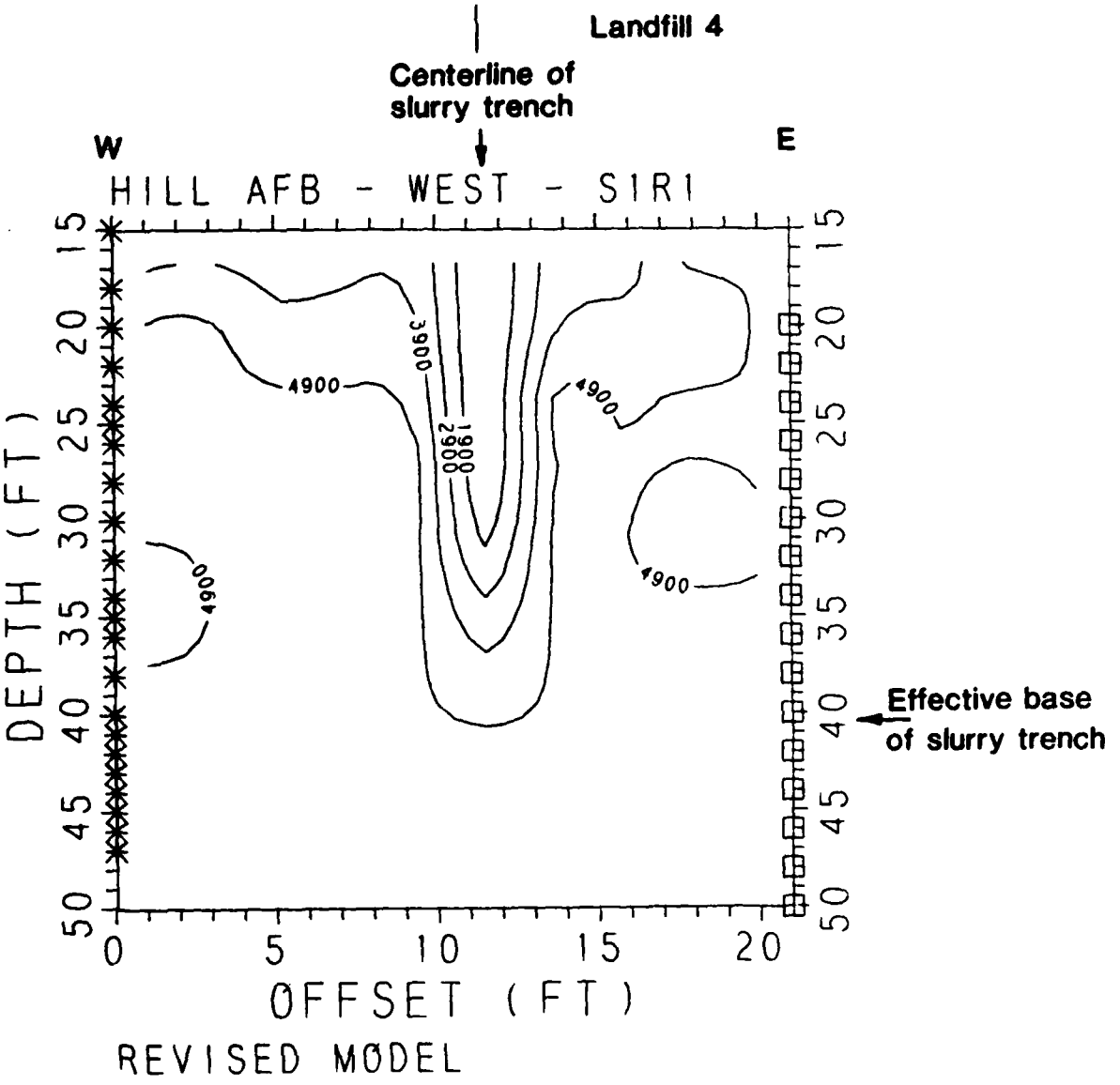

Figure 17. Revised tomographic model, west location.

3.4.4 Boreholes S-4 and M-21

East of Landfill 4 only one deep hole was available - shot hole S-4 12 feet south of monitoring well M-22 [see Figure 1]. This hole was 50 feet deep. In order to image the base of the slurry trench, we shot into 6 geophones placed in monitoring well M-21 at 2 feet intervals from 19 feet to 29 feet depth [see Figure 18]. The measured distance between S-4 and M-21 was 22 feet, with the estimated center of the slurry trench falling midway between the boreholes. In an attempt to increase the number of raypaths and improve the resolution, the shots were also recorded using an additional 12 geophones laid out on the surface between S-4 and M-21.

First break picks on the surface traces were difficult to make with confidence because of a high level of background noise and also because casing breaks, travelling up the shot casing, came in before the direct arrivals on the geophones near S-4. The events were also low in amplitude because of attenuation in the unsaturated surface layer. On the borehole traces, clear first breaks were only shown on the lower two geophones and these rapidly decreased in amplitude for shots above a depth of 35 feet. However, a water wave was visible on all the geophone records, indicating water in M-21 to above 19 feet.

Since the data are limited, the choice of initial model for the inversion is important. Several trials were performed with different starting models to find the one which gave the best initial fit to the data. This model consisted of a water table at 18 feet separating material with P-wave velocity of 1,500 ft/sec above and 5,000 ft/sec below. A low-velocity [1,000 ft/sec] column at the location of the slurry trench extended from 18 feet to 42 feet depth.

Upon iterating on this model, using curved rays, the results shown in Figure 18 were obtained. The main change from the starting model is that the low-velocity region marking the slurry trench has shallowed from 42 feet to near 39 feet. Figure 19 shows the raypaths

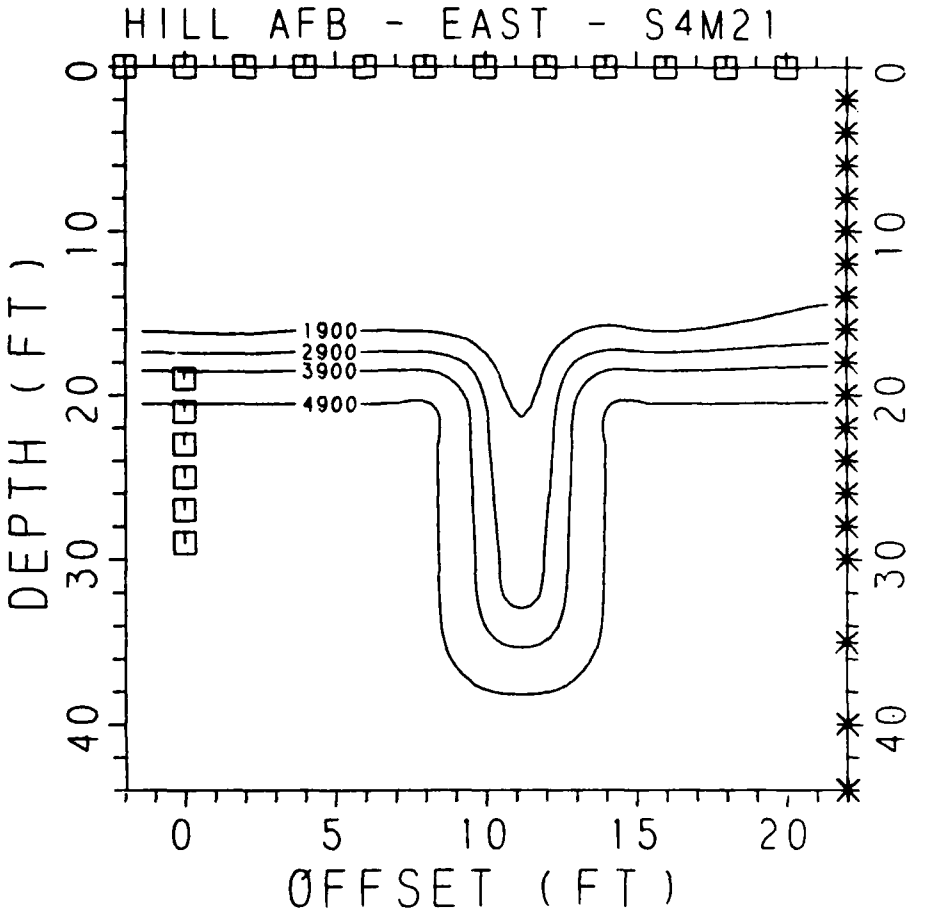

Figure 18. Shot-receiver geometry and tomographic inversion, east location.

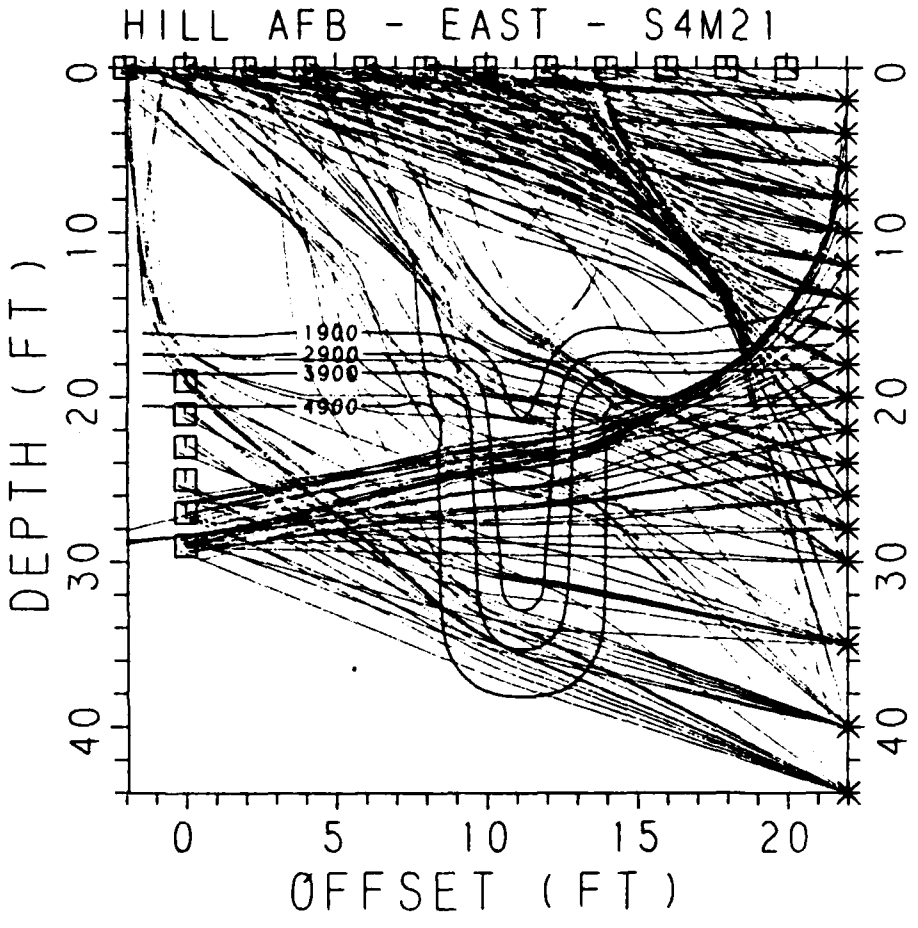

Figure 19. Curved raypaths through inversion model, boreholes S-4/M-21.

corresponding to this model. The rays are highly curved, particularly at the water table boundary. Notice also that the rays concentrate in certain regions of the model, giving rise to 'shadow zones' where few rays penetrate. This is possibly the reason why direct arrivals appear to be absent on the top four borehole geophones; these geophones lie in a shadow zone created by the slurry trench and the water table.

Since relatively few rays cross the slurry trench below 35 feet, the interpretation of 39 feet as the effective base of the trench is tentative. Figure 20 shows the seismic traces for the deepest borehole receiver and shots from 20 to 44 feet depth. A diffraction depth of 41 feet can fit an apparent diffracted event following the first breaks, and direct arrivals at 5,000 ft/sec can fit the first breaks for the two deepest shots, if a borehole separation of 18 feet, rather than 22 feet, is assumed. These values are not, therefore, inconsistent with a termination of the trench near 40 feet depth. However, because of the limited ray coverage at this depth, we cannot exclude the possibility that the trench extends deeper.

4.0 CONCLUSIONS

The seismic data appear to indicate that the unsaturated portion of the slurry trench terminates between 35 and 40 feet depth at the three locations tested. With reasonable constraints, the tomography approach appears to work well in delineating this depth and also in identifying other unsaturated zones that may represent more silty areas. Because of the tendency of the tomographic inversion method to smear out velocity anomalies between the boreholes, additional dynamite shots fired along the surface between the boreholes should be included in any future tomography surveys performed at this site.

5.0 REFERENCES

Worthington, M.H., 1984, An Introduction to Geophysical Tomography, First Break, 2, No. 11, p. 20-26.

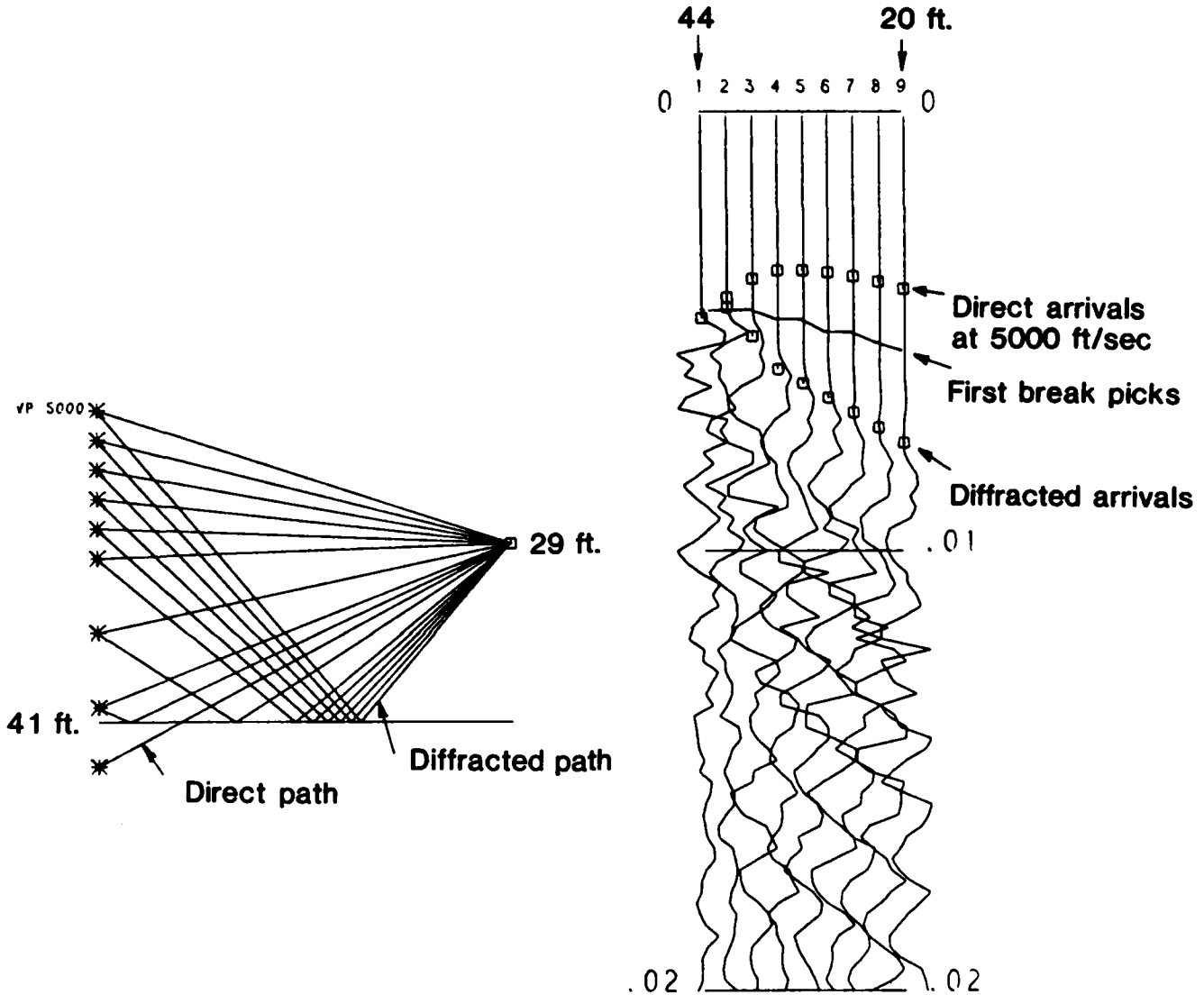

Figure 20. Raypaths and identified arrivals at deepest receiver, east location.

END

7-87

DTIC